Eur Biophys J (1988) 16:73–81

European Biophysics Journal

Orientation of the tryptophans responsible for the photoinactivation of nerve sodium channels

F. Conti [1] *, A. M. Cantú [1], and H. Duclohier [2]

[1] Istituto di Cibernetica e Biofisica del CNR, I-16032-Camogli, Italy
[2] Laboratoire de Chimie Macromoléculaire, Université de Rouen, F-76130 Mont Saint Aignan, France

Received October 5, 1987/Accepted in revised form January 5, 1988

Abstract. UV irradiation of squid giant axons at wavelengths of 280 or 290 nm produces nearly the same rate of irreversible decrease of sodium currents. The rate of photodeactivation is unaffected by extensive removal of axoplasm with pronase, and it is independent of temperature in the range 5° to 20 °C. The photochemical effect appears to be all or nothing. It does not alter the time course and the voltage dependence for activation and inactivation of the residual currents. Similar deactivation rates were produced by irradiations of the same intensity, but linearly polarized either parallel or perpendicular to the axon. The efficiency of the deactivation process is close to that expected if it was caused by the photooxidation of a single tryptophan residue per sodium channel. Owing to the geometry of the preparation the lack of polarization asymmetry suggests that this residue assumes nearly random (or pseudo-random) orientation in the three-dimensional structure of the sodium channel corresponding to the closed state.

Key words: UV damage, sodium channels, axon, UV absorption, polarization, tryptophan

Introduction

It has long been established (Booth et al. 1950; Lieberman 1967) that the damage produced by UV radiation on nerve excitability is maximal at wavelengths characteristic of photon absorption by aromatic amino-acid residues (Wetlaufer 1962). In voltage-clamped preparations of myelinated nerves (Fox and Stampfli 1971; Fox 1974a, b, 1976; Fox et al. 1976; Schwarz and Fox 1977; Hof and Fox 1983, 1984) and lobster axons (Oxford and Pooler 1975) the effect has been shown to involve primarily the sodium channels. In skeletal muscle fibres, recovery from localized photodestruction of sodium and potassium channels has been used to estimate the lateral mobility of these membrane proteins (Stuehmer and Almers 1983; Weiss et al. 1986). Gramicidin A channels in artificial bilayers are also altered by UV light, with maximal sensitivity at 280 nm, due to photochemical reactions involving the tryptophan residues, and this effect has been used to gain information about the influence of these residues on the formation of the channel pore and on its properties (Busath and Waldbillig 1983; Jones et al. 1986).

The primary sequences of the sodium channel in the electric eel, *Electrophorus electricus* and in rat brain have been recently elucidated by Numa and coworkers (Noda et al. 1984, 1986) and this has led to the formulation of models for the three-dimensional structure of the channel (Noda et al. 1984, 1986; Kosower 1985; Greenblatt et al. 1985; Guy and Seetharamulu 1986). All these models attribute crucial roles for the channel function to transmembrane α-helices which contain only a few tryptophan residues. In agreement with these models, we shall argue here that the photoinactivation of the sodium channels may indeed result from the photooxidation of just one tryptophan residue.

Sodium currents in squid giant axons can be measured with great accuracy and the photochemical effect in this preparation can be exploited for quantitative studies of absorption spectroscopy of the crucial photoreactive centres. In the present study we take advantage of the simple geometry of the squid giant axon to gain information about the orientation of these centres by irradiating the axon with polarized light. Because of the use of a continuous light source, to obtain a sufficient rate of polarized UV irradiation of large membrane areas, this information concerns only the closed (resting) configuration of the sodium channel.

* To whom offprint requests should be sent

Methods

Axon preparation

Single giant axons were isolated from the hindmost stellar nerve of the squid *Loligo vulgaris* available in Camogli. The axons were freed of all adjacent small fibres for a length of about 30 mm and placed horizontally in a perspex chamber. The latter followed a standard design (Conti et al. 1982) except for the top of the cell, which was provided by a small quartz cylindrical lens (plano-convex, focal length in water 12 mm), placed with the flat surface in direct contact with the extracellular solution and with its symmetry axis parallel to the axon.

The axons were impaled with "piggy-back" electrodes (Chandler and Meves 1965) comprising a platinized platinum wire as current electrode (18 mm exposed), and a glass pipette (filled with 0.5 *M* KCl, and connected to an Ag-AgCl electrode) to measure the intracellular potential. The extracellular current electrodes were platinized platinum foils glued to the movable lateral walls of the chamber. Each side wall contained a virtual ground central electrode (4 mm × 6 mm) for the current measurement and two grounded lateral guard-electrodes of the same size. The walls were widely separated during the preliminary operations and were positioned at about 2 mm on each side of the axon before starting the measurements.

The extracellular voltage was probed with an Ag-AgCl electrode via polyethylene tubing approaching the centre of the axon from the bottom. The extracellular medium bathing the axons was artificial sea water (ASW) with the following composition: 450 m*M* NaCl; 10 m*M* KCl; 50 m*M* $CaCl_2$; 10 m*M* *Tris*Cl (pH = 7.8).

In perfused preparations the intracellular solution had the following composition: 300 m*M* CsF; 20 m*M* Na-phosphate buffer (pH = 7.3); 20 m*M* TEACl; 400 m*M* sucrose. The temperature was measured with the aid of a small thermistor placed near the axon and was regulated by a Peltier cell (Cambion, Cambridge, Mass).

Voltage-clamp apparatus

The voltage-clamp circuit followed a standard configuration (Moore and Cole 1963), except for a time-lag of about 10 or 20 μs which was introduced in the positive feed-back for the compensation of the series resistance, R_s (Hodgkin et al. 1952). This allowed 100% compensation of the estimated R_s, avoiding undesired oscillations owing to the fact that at high frequencies the impedance of access to the axon membrane is not equivalent to a simple resistor (Benz and Conti 1981). As discussed extensively by Kimura and Meves (1979), an accurate compensation of R_s is crucial for a correct comparison of I-V characteristics showing large differences in peak current amplitudes.

An estimate of the effective low-frequency value of R_s was obtained by extrapolating to time zero the linear voltage increase between 50 and 200 μs from the application of a step of constant current. We found specific values of R_s varying between 2.7 and 4.3 Ω cm^2, in good agreement with the estimates of Salzberg and Bezanilla (1983) obtained using an independent optical method.

The adequacy of our compensation was checked in several experiments by verifying that the voltage dependence of peak sodium currents was not modified when the currents were reduced several-fold upon addition of 10 n*M* tetrodotoxin to the extracellular medium.

Optical set-up

The light source was a high pressure mercury arc lamp (HBO 200 W, OSRAM) placed in a lamp housing with quartz optics (ORIEL mod. 20080). The wide parallel beam of light formed by the condenser in the lamp-housing was first filtered and then reflected toward the axon chamber by a surface-aluminized mirror. The cylindrical lens on top of the chamber partly focused the light onto the axon without significant modification of the relevant polarization properties of the incoming photons. The irradiated length of the axon was about 20 mm. Electrophysiological measurements of the photochemical effects were obtained from a central region of about 6 mm.

Narrow-band radiation was obtained by use of interference filters with peak transmissions (19%) at 280 nm or at 290 nm and half-widths of about 5 nm (IR Ind., Waltham, Mass.). Polarized light was obtained by inserting a linear polarizer (Polaroid HNP'B) with suitable orientation in the path of the irradiating beam immediately before the cylindrical lens.

The intensity, W, of the radiation illuminating the axon, was estimated to be 1.8 mW cm^{-2} when the 280 nm filter and no polarizer were used. With the 290 nm filter W was about 1.2 mW cm^{-2}. The polarizer reduced the intensity of the beam to about 20% of its original value. These estimates were in good agreement with the expectations from the specifications of the spectral characteristics and transmission efficiencies of the optical components.

Stimulation and data acquisition

The start and finish of light stimulation was hand-controlled. Electrical stimulation and the acquisition

of membrane current was performed with the aid of a PDP 11/23 computer. The data were acquired digitally at 10 or 20 μs sampling intervals after filtering (low-pass 8-pole Bessel with 16 KHz cut-off).

Each record was corrected for unspecific linear responses estimated from a P/4 stimulation protocol with smaller control pulses from a holding potential of −120 mV (Armstrong and Bezanilla 1977). All relevant information concerning the stimulation protocol, including the real time of acquisition of each record, was stored on file.

Three types of stimulation sequences were used: a) I–V sequences, consisting of several depolarizations to various test potentials, Em, starting from a holding potential, Eh, of −90 mV; b) h_∞ sequences, consisting of several depolarizations to the same test potential from different prepulse potentials, Ep, maintained for 30 ms; c) photodeactivation sequences consisting of repeated identical stimulations (Eh = −90, Em = 0) at constant time intervals (2–5 s). The first two sequences were applied only during "dark" periods. The third was used to monitor the continuous decrease with time of the sodium currents during UV irradiation.

The peak sodium current, Ip, was defined for each stored record as the minimum of a third-order polynomial least-squares fitted to an appropriate interval of the sampled data.

Results

General features

Figure 1 shows several successive records of sodium currents obtained from repeated identical step depolarizations of a squid giant axon before, during, and after a continuous UV irradiation period of 110 s at 280 nm and 1.8 mW cm^{-2}. It is seen that records taken during dark periods (1 to 4 and 8 to 12), are practically indistinguishable. In this, as in most of our experiments, sodium currents were monitored every 5 s, but for clarity the figure shows only one out of every five recordings. For a total irradiation dose such as that of Fig. 1, producing about 20% photoinactivation, the amplitude of the sodium currents appears to decrease linearly with time.

More prolonged irradiation produced a clearly exponential decay, in agreement with the reports of several authors on other preparations (Fox 1974a; Oxford and Pooler 1975; Weiss et al. 1986). In most experiments we avoided such extensively destructive doses under any fixed condition, because they are not required for the measurements of photoinactivation rates, whereas they do prevent one from obtaining several such measurements and other information (polarization, etc.) from the same axon.

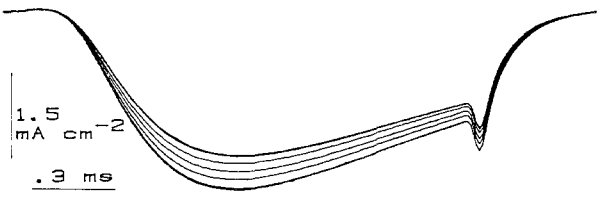

Fig. 1. Successive recordings of voltage-clamp currents from an intact axon in response to voltage steps to 0 mV from a holding potential of −90 mV. Bandwidth: 16 kHz. Temperature: 7.5 °C. The figure shows the superimposition of a total of 12 records, but the individual records within the first group of 4 and within the last group of 5, taken respectively before and after 110 s of UV irradiation at 280 nm and 1.8 nW cm^{-2}, are indistinguishable from each other. Records 5 to 8 show the decay of sodium currents monitored every 20 s after the onset of the UV irradiation, starting in coincidence with record 4 and ending with record 8

The effect shown in Fig. 1 occurred with no obvious delay either at the onset or at the termination of the UV stimulation. Furthermore we could never detect any significant fast component of the decay of the type reported by Jones et al. (1986) for the photolysis of tryptophan residues in the gramicidin channel. Despite the poor time resolution for our control of the onset of UV irradiation, the latter statement stands on firm ground because the time course of Ip measurements never showed any appreciable discontinuity near the onset of any UV irradiation period (see Figs. 4 to 6).

Apart from the decreased amplitude the records of Fig. 1 obtained before and after the irradiation period have the same time course and could be made to overlap simply by using a scaling factor, as if the only effect of the irradiation was the disappearance of about 20% of the sodium channels while the properties of the others were unaffected. This conclusion was further supported by the observation that the activation and inactivation properties of the sodium currents which survived prolonged irradiation periods were not significantly different from those measured before irradiation.

Figure 2 shows the comparison between the I–V characteristics of a fresh axon and that obtained from the same axon after a loss of about 40% of the sodium currents produced by two irradiation periods of 110 s at 280 nm and one at 290 nm. It is seen that, apart from a normalization factor, the two data sets are practically identical.

The same is true for the voltage dependence of the inactivation, shown for the same axon in Fig. 3.

Inactivation rates

The time course of the decrease of peak sodium currents during UV irradiation is shown in Fig. 4. Up-

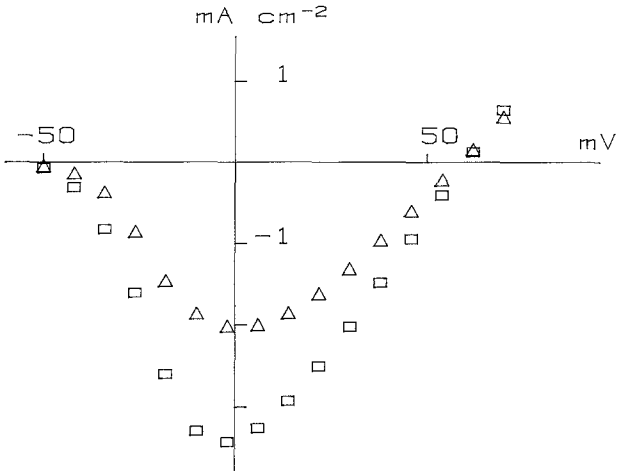

Fig. 2. UV irradiation does not affect the voltage dependence of the residual sodium currents. *Open squares*: Peak sodium currents measured in a fresh axon before UV irradiation, the stimulation protocol consisted of 16 depolarizations from a holding potential of −90 mV to membrane potentials increasing in steps of 8 mV, from −50 mV to 70 mV. *Open triangles*: Similar measurements in the same axon after two periods of UV irradiation at 280 nm and one period of irradiation at 290 nm. The two sets of data can be made to superimpose by a scaling factor of 1.7 (T= 8 °C)

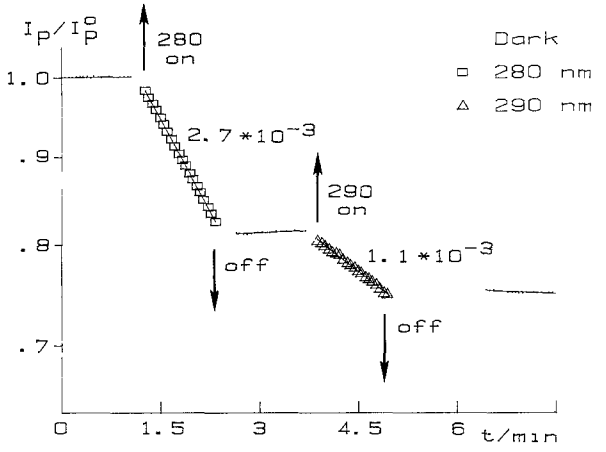

Fig. 4. Time course of peak sodium currents in response to repeated identical stimulations (from Eh = −90 mV to Em = 0 mV) during three dark periods interspersed by periods of UV irradiation at 280 nm and 290 nm. The peak current density measured at time zero, I_p^0, was 3.3 mA cm^{-2}. The ratio I_p/I_p^0 is plotted on a semilogarithmic scale against time. The estimated light intensity during the continuous irradiation was 1.8 mW cm^{-2} at 280 nm and about 35% lower at 290 nm. The indicated K_d values for the irradiation periods are in unit of s^{-1} and they were obtained from least-squares fits of the data according to Eq. (1) (*continuous lines*)

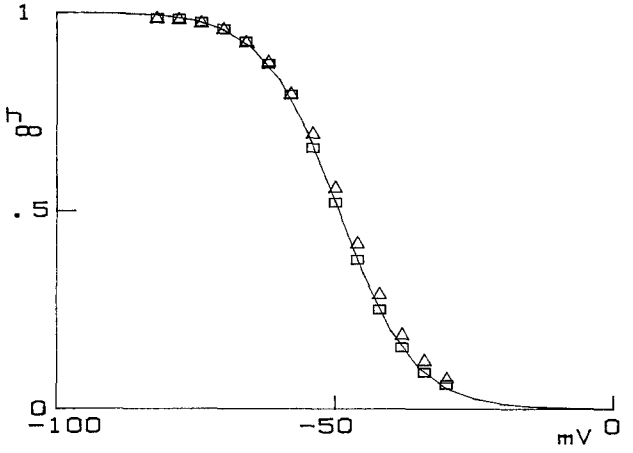

Fig. 3. Lack of effect of UV radiation on the voltage dependence of the inactivation of sodium channels (h_∞). Peak sodium currents for pulse depolarisations to 0 mV are plotted against the value of the prepulse potential, Ep, lasting 30 ms. The data are normalized to the peak current measured with no prepulse (Ep = Eh = −90 mV). *Open squares*: data from a fresh axon; *open triangle*: data from the same axon after three irradiation periods, which reduced the peak currents by about 40%. Same experiment as Fig. 2. (T= 8 °C). The solid line shows the least-square fit of the data to the equation:

$$h_\infty = 1/\left[1 + \exp\frac{V - V_0}{V_h}\right],$$

where $V_0 = -49$ mV and $V_h = 6.5$ mV

ward and downward arrows indicate, repectively, the start and the end of two 110 s periods of UV irradiation, the first at 280 nm and the second at 290 nm. The decay of I_p with time, t, during the irradiation at 280 nm was least-squares fitted to the equation:

$$I_p/I_p^0 = \exp(-K_d(t - t_0)), \quad (1)$$

where t_0 is the start time of irradiation, I_p^0 is the peak current at t_0 and $K_d = 2.7 \times 10^{-3}$ s^{-1}. A similar fit of the decay of I_p during irradiation at 290 nm yielded $K_d = 1.1 \times 10^{-3}$ s^{-1}.

In this experiment the fit of Eq. (1) to the data obtained during the dark periods yielded K_d values more than two orders of magnitude smaller. In general, drifts of I_p during dark periods could be described as "background noise" of the order of few percent in our K_d measurement. In three axons, successive measurements of K_d at 280 and 290 nm, as in Fig. 4, yielded the following ratios between the two rates: 2.0, 2.2 and 2.4.

Considering the difference in the intensity of the two irradiations, we estimate that the efficiency of photodeactivation at 280 nm is about 1.5 times larger than at 290 nm, a result which is in good agreement with that reported for frog nodes (Fox 1974a), for lobster axons (Oxford and Pooler 1975), and for skeletal muscle fibres (Weiss et al. 1986). A ratio of 1.4 between the absorption efficiencies at 280 nm and at

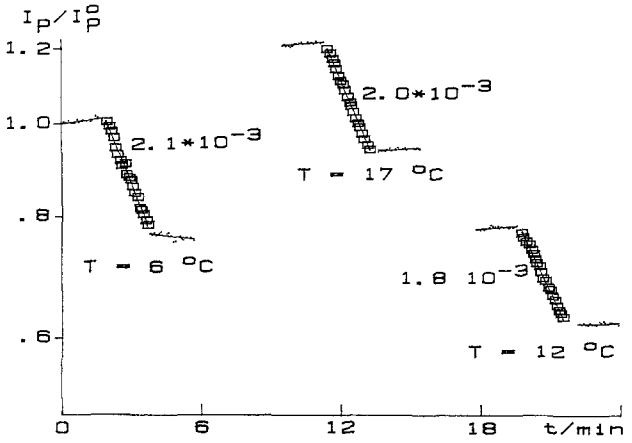

Fig. 5. The independence of denaturation rates on temperature. The decay of peak sodium currents with time is measured on the same axon at the three temperatures indicated. The experimental conditions are similar to those of Fig. 5. The three irradiation periods lasted 110 s each. The wavelength of irradiation was 280 nm, the intensity was about 1.8 mW cm^{-2}. The peak current at the beginning of the experiment ($t = 0$) was 2.4 mA cm^{-2}. Notice the discontinuities of I_p associated with the changes in temperature ($Q_{10} \simeq 1.7$). K_d values for each irradiation, obtained from least-squares fit of Eq. (1) to the data are given in units of s^{-1}

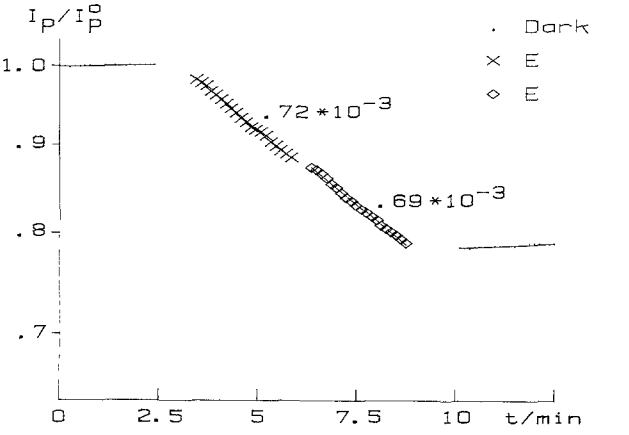

Fig. 6. Lack of polarization effects on the UV-inactivation of sodium channels. The same axon is irradiated with 280 nm photons polarized either parallel (*open squares*) or perpendicular (*crosses*) to its axis. The denaturation rate is the same in the two cases. The K values, in units of s^{-1}, are lower than in Fig. 5 because the polarizer absorbs about 80% of the light available after the interference filter. However, the intensity of the light source was increased in this case by about 40% by driving the lamp at a power higher than nominal

290 nm is expected for tryptophan, whereas the same figure for tyrosine is about 12 (Wetlaufer 1962).

A direct correlation between photodeactivation and tryptophan absorption was also established by exciting the fluorescence of tryptophan solutions with the same optical setup used for irradiation of the axons. The solutions were inserted in a quartz tube of about 1 mm diameter, positioned in the axon chamber as a model axon. The ratio between the fluorescence emitted by the tube upon excitation at 280 nm or 290 nm was about 2.1, very close to the ratio of the inactivation rates of Fig. 4.

For similar experimental conditions the K_d values measured in seven axons under 280 nm irradiation varied in the range $(1.8 - 2.7) \times 10^{-3}$ s^{-1}. Some of this variability might be due to variations in the power absorbed by the arc lamp. However, we cannot exclude some influence of differences in geometrical parameters such as the diameter and the position of the axon, which may affect the results if the irradiating beam is not uniform.

The inactivation rates were found in three experiments to be fairly independent of temperature in the range from 6° to 20 °C. Figure 5 shows three successive runs of measurements such as that of Fig. 4, performed successively at 6°, 17° and 12 °C. An apparent slight decrease of K_d following the first temperature change was followed by a similar decrease after the second change in temperature of opposite sign. Most probably, these decreases arise from non-uniformities of the irradiating beam which lead to a photoselection of different membrane areas during prolonged irradiations. Higher K_d's from membrane areas which are more brightly illuminated will be emphasized initially, but their contribution will decrease at later times because of the faster decay of sodium channel activity in these regions.

The independence of K_d on temperature is in agreement with the results of Fox (1974a) on frog nodes and with those of Weigele and Barchi (1980) on the loss of saxitoxin binding produced by UV irradiation of sodium channels in rat synaptosomes.

Polarization measurements

In three different experiments we tried to detect differences in the rate of photodenaturation produced by exciting photons of different polarization. By introducing the polarizer in the path of the exciting beam, K_d decreased by a factor 5, consistent with an effective 20% transmission of the polarizer and a linear dependence of the UV effect on the light intensity due to the "single hit" nature of the photodenaturation process. In some runs such as that shown in Fig. 6, the attenuation of the polarizer was partially compensated by driving the arc-lamp at a power 50% higher than the nominal.

K_d was found to be independent of the orientation of the polarizer. It is seen that no significant changes in

K_d occur when the polarization of the exciting photons is switched from parallel to perpendicular to the axon and vice-versa. Controls to show that the intensity of the parallel and perpendicular irradiations were identical, i.e. that the light beam before the polarizer had no polarization asymmetries, were performed by testing the fluorescence of tryptophan solutions as described before.

Discussion

Most of the general features of the photodenaturation of sodium channels that we have found in the present work agree with previous studies of the same effect in other preparations. These include: the proportionality between the denaturation rate and the UV light intensity, which implies a single photon effect (Fox and Stampfli 1971; Hof and Fox 1983; Weigele and Barchi 1980); the similarity of the effects produced by 280 and 290 nm radiations (Fox 1974a; Oxford and Pooler 1975; Weigele and Barchi 1980; Weiss et al. 1986); and the independence of the effect on temperature (Fox 1974a; Weigele and Barchi 1980). The "all or nothing" character of the UV effects is in agreement with what has been reported by Oxford and Pooler (1975) for lobster axons and by Weiss et al. (1986) for skeletal muscle fibres. The more complex phenomenology reported for frog nodes, where significant shifts in the inactivation of the residual sodium currents are observed (Fox 1976; Schwarz and Fox 1977; Hof and Fox 1983), seems to be peculiar to this preparation. Indeed, these effects, which are most prominent for irradiations at 260 nm and are sensitive to the action of sulfhydryl compounds (Hof and Fox 1984), have been attributed to modifications of the membrane surface-charge rather than to alterations of the channel proteins. The simplest kinetic scheme accounting for the irreversible photochemical denaturation of the sodium channels is given by:

$$C \underset{hvq}{\overset{k}{\leftrightarrows}} C^* \xrightarrow{\alpha_d} C_d \qquad (2)$$

where C represents a native sodium channel; C^* is the excited state produced by the absorption of a UV photon by a reactive group; α_d is the rate of decay to the denatured state, C_d; and k is the total rate of all the other possible decays of C^* to the ground state. The rate q of the transition from C to C^* is given by the product of the effective absorption cross section of the reaction centres, σ [cm^2/photon], and the intensity of the photon flux, I [photons $cm^{-2}\,s^{-1}$].

From the extinction coefficient of tryptophan in bulk solutions (Wetlaufer 1962) the absorption cross section of a single tryptophan residue for photons of 280 nm can be estimated to be of the order of $2 \cdot 10^{-17}$ cm^2 [1]. Since the energy of a photon at 280 nm is about $7 \cdot 10^{-19}$ J, the irradiation rates used in this work ($W = 1.8$ mW cm^{-2}) correspond to about $2.7 \cdot 10^{15}$ photons $cm^{-2}\,s^{-1}$. Thus, assuming n effective reactive centres per sodium channel, the rate q in reaction (2) is of the order of $0.054\,n\,s^{-1}$.

Since the time constants for the fluorescent decay of aromatic residues, either isolated or in proteins, are of the order of a few nanoseconds (Beechem and Brand 1985) the total rate of non-denaturing decays from state C^* is expected to be at least of the order of $10^8\,s^{-1}$, so that, in any case: $k \gg q$. Using this condition it is simple to verify (see Appendix A) that the scheme (Eq. (2)) predicts a simple exponential decay of the number of native channels with a rate constant, K_d, given by:

$$K_d = \Phi_d \cdot q \qquad (3)$$

where:

$\Phi_d = \alpha_d/(\alpha_d + k)$

is the efficiency of the photochemical denaturation.

Comparing the above estimates of q with our measured values of K_d ($2.2 \cdot 10^{-3}\,s^{-1}$ for $W = 1.8$ mW cm^{-2}) we obtain from Eq. (3) an estimate of Φ_d of about $0.04/n$.

For $n = 1$ this value is very close to the efficiency of photooxidation of tryptophan residues (Creed 1984; Busath and Waldbillig 1983), suggesting that indeed only the photolysis of one or a few particular tryptophans prevents the sodium channel from functioning.

Consistent with the above conclusion, it should be noticed that in the amino acid sequence of the sodium channel of *Electrophorus electricus* only one of the 31 Trp residues present, (Trp 671) is located within one of the segments (S4, repeat II), which have been modelled by Noda et al. (1984) as having a crucial role in the channel function, whereas in the model proposed by Kosower (1985), the four other Trp residues (1066, 1068, 1140, 1385) which are assigned to hydrophobic transmembrane helices (H7, H8, H12) are relatively remote from the ion-pore.

Further circumstantial support for the idea that only one tryptophan is responsible for photoinactivation is provided by the all-or-nothing nature of the phenomenon, which is in contrast with the wide spectrum of effects observed in the case of gramicidin A where several equivalent residues are involved (Busath and Waldbillig 1983).

---

[1] This figure can be obtained from the molar extinction coefficient, $\varepsilon_m = 5.5 \cdot 10^3\,M^{-1}\,cm^{-1}$ at 280 nm and from the relation (see also Busath and Waldbillig 1983):

$\sigma = 2.3 \cdot 10^3 \cdot \varepsilon_m/N_A$,

where N_A is Avogadro's number

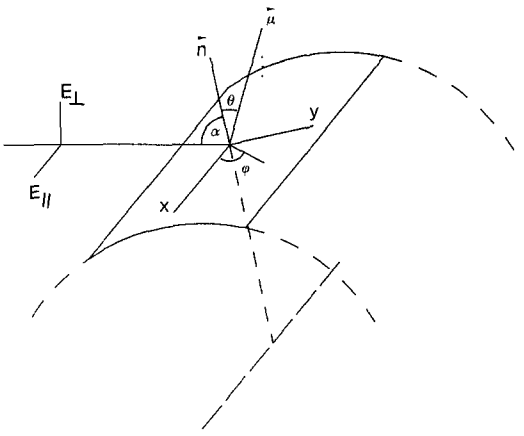

Fig. 7. Scheme of the absorption of photons by a chromophore bound to a sodium channel in the axon membrane. $\boldsymbol{n}$ is the normal to the membrane at the location of the chromophore. The x and y axes, are on the plane tangential to the axon surface. α is the angle between the direction of incidence of the light and $\boldsymbol{n}$; $\boldsymbol{\mu}$ is the absorption dipole moment of the chromophore, which forms the angle Θ with $\boldsymbol{n}$; φ is the angle between the x axis and the projection of $\boldsymbol{\mu}$ onto the xy plane. $E_{\parallel}$ and $E_{\perp}$ respectively indicate the electric vector of incoming polarized parallel and perpendicular respectively to the axon

Following the above considerations it is interesting to discuss the data on polarized irradiation assuming a single photodeactivation centre and an ideal cylindrical geometry for the axon membrane. The latter assumption is well supported on several grounds. First, departures from local membrane planarity on the micron scale are observed in electromicrographs of giant axons only occasionally and they are much less frequent in freeze-fractured replicas, which are less subject to fixation artifacts (Villegas and Villegas 1984). Second, should membrane foldings be extensive in vivo, they would increase significantly the effective membrane area, making the apparent specific capacity of the squid axon membrane much higher than that of solvent-free lipid bilayers, just the opposite of what is actually observed (Haydon et al. 1980). Finally the strong polarisation anisotropy of the optical changes observed in squid axons stained with fluorescent dyes is inconsistent with a random orientation of the axon membrane, whereas it is very well accounted for by a simple cylindrical geometry (Conti 1975).

For the above simple model it is easy to express the dependence of the rate q in Eq. (2) on the orientation of the absorption dipole with respect to the irradiating beam. If the chromophore is rigidly attached to the channel protein and if the latter can be viewed as a rigid structure which is only free to translate along the plane of the membrane and to rotate around the normal to this plane, $\boldsymbol{n}$, the absorption dipole $\boldsymbol{\mu}$ of our chromophore is expected to form with $\boldsymbol{n}$ a fixed angle, Θ, while the orientation of its projection on the plane of the membrane is expected to be completely random (see Fig. 7).

Let $q_{\parallel}$ and $q_{\perp}$ be, respectively, the rate of absorbtion of photons with the electric vector, $\boldsymbol{E}$, parallel or perpendicular to the axon. We shall have:

$$q = q_{\parallel} + q_{\perp} . \tag{4}$$

Furthermore, as shown in Appendix B:

$$q_{\parallel} = (1/2)\,\sigma_0\, I_{\parallel} \sin^2 \Theta \tag{5}$$

$$q_{\perp} = (1/2)\,\sigma_0\, I_{\perp} [\cos^2 \Theta + (1/2)\sin^2 \Theta] , \tag{6}$$

where $I_{\parallel}$ and $I_{\perp}$, respectively, are the fluxes of photons polarized parallel or perpendicular to the axon; and σ_0 is the cross section offered by a chromophore when its absorption dipole is parallel to E. σ_0 is related to the mean cross section, σ, of randomly oriented chromophores in the bulk phase by: $\sigma_0 = 3\,\sigma$.

For excitation with unpolarized photons ($I_{\parallel} = I_{\perp} = I/2$):

$$q = (1/4)\,\sigma_0\, I\,[1 + (1/2)\sin^2 \Theta] \tag{7}$$

The ratio of the absorption efficiencies for orthogonally polarized irradiations of the same intensity is given by:

$$q_{\perp}/q_{\parallel} = (1/2) + \cot g^2\, \Theta . \tag{8}$$

This ratio can assume any value between 0.5 and ∞ and it becomes unity for the particular case of $\Theta \sim 55°$.

On the other hand, if the absorbing chromophores have random orientations, the mean absorption rates are obtained from Eqs. (5) and (6) after averaging over Θ (with the weighting factor $\sin \Theta\, \mathrm{d}\Theta$). In this case, for $I_{\parallel} = I_{\perp} = I/2$:

$$q_{\parallel} = q_{\perp} = (1/6)\,\sigma_0\, I. \tag{9}$$

The absorption is then independent of photon polarization and the effective cross section, $\sigma = (q_{\parallel} + q_{\perp})/I$, is $\sigma_0/3$ as in bulk solutions.

The above discussion suggests that the lack of polarization asymmetry observed in our measurements is simply due to a random orientation of the tryptophans responsible for the photoinactivation of a sodium channel. Such a situation is more likely to arise from freedom of the residues to reorient themselves relative to the channel backbone than from allowed rotations of the whole protein around an axis parallel to the membrane surface.

However, we cannot exclude that either by mere fortuitous coincidence the relevant chromophores have a mean orientation with Θ close to 55°, or that more photoinactivation centres coexist in each sodium channel with fixed complementary orientations.

Finally it should be stressed that all our conclusions apply only to the closed configuration of the

sodium channel, which is by far the most populated at $E_h = -90$ mV. Different results might be expected for the open conformation, since Hof and Fox (1983) have reported that the efficiency of flash irradiations of frog nodes depends on the electrophysiological state of the nerve. Such dependence may arise from differences in the lifetime of the tryptophan's excited state. However, Eq. (7) shows that the efficiency of photodenaturation may also change significantly because of variations in the mean orientation of the reactive chromophores.

Appendix A

Let N and N^*, respectively, denote the number of sodium channels in the native state and in the excited state. Their time course, according to the kinetic scheme (2), is governed by the linear differential equations:

$$dN/dt = -q N + k N^* \tag{A1}$$

$$dN^*/dt = qN - (k + \alpha_d) N^* . \tag{A2}$$

The solution of the above equations is:

$$N(t) = a_1 e^{-\lambda_1 t} + a_2 e^{-\lambda_2 t} \tag{A3}$$

where λ_1 and λ_2 are the roots of the secular equation:

$$\lambda^2 - (k + \alpha_d + q)\lambda + q\alpha_d = 0 \tag{A4}$$

or:

$$\lambda = \frac{(k + \alpha_d + q) \pm \sqrt{(k + \alpha_d + q)^2 - 4\alpha_d q}}{2} . \tag{A5}$$

For $q \ll k$ we have:

$$4\alpha_d q \ll 4\alpha_d k < 2\alpha_d k + k^2 + \alpha_d^2 < (k + \alpha_d + q)^2$$

and:

$$\sqrt{(k + \alpha_d + q)^2 - 4\alpha_d q} \sim (k + \alpha_d + q) \cdot \left[1 - \frac{2\alpha_d q}{(k + \alpha_d + q)^2}\right].$$

Using the above approximation the rates λ_1 and λ_2 are given by:

$$\lambda_1 \sim k + \alpha_d \tag{A6}$$

$$\lambda_2 \sim q\alpha_d/(k + \alpha_d) \tag{A7}$$

The coefficients a_1 and a_2 in Eq. (A3) are obtained by imposing the initial conditions:

$$a_1 + a_2 = N(0) \tag{A8}$$

$$a_1\lambda_1 + a_2\lambda_2 = -\left.\frac{dN}{dt}\right]_0 = q N(0) \tag{A9}$$

From that last two equations we have:

$$a_1/a_2 = (q - \lambda_2)/(\lambda_1 - q) \tag{A10}$$

and inserting the values of λ_1 and λ_2 from Eqs. (A6) and (A7):

$$a_1/a_2 \sim \frac{q k}{(k + \alpha_d)^2} < \frac{q}{k + \alpha_d} \ll 1 .$$

Thus the fast component of the decay of $N(t)$, with the rate λ_1 yields only a trivial contribution in Eq. (3), which can be for all practical purposes replaced by:

$$N(t) = N(0) e^{-K_d t} \tag{A11}$$

where:

$$K_d = \lambda_2 = q\alpha_d/(\alpha_d + k) \tag{A12}.$$

Appendix B

Let us consider the absorption properties of a chromophore in a sodium channel situated at a point in the axon membrane characterized by the angle α, and let φ and Θ be the angles characterizing the orientation of its absorption dipole, $\boldsymbol{\mu}$ with respect to a local system of coordinates having $\boldsymbol{n}$ as z axis and the x axis parallel to the axon (Fig. 7).

If the chromophore is exposed to a flux of exciting photons, I, having the electric vector, $\boldsymbol{E}$, parallel to the axon, the rate of photon absorption per unit time, $\Phi_{\parallel}(\varphi, \Theta)$, is independent of α and given by:

$$\Phi_{\parallel}(\varphi, \Theta) = \sigma_0 I_{\parallel} \sin^2\Theta \cos^2\varphi , \tag{B1}$$

where σ_0 is the maximum cross section for absorption, obtained when $\boldsymbol{\mu}$ is parallel to $\boldsymbol{E}$.

Similarly, for a flux, $I_{\perp}$, of exciting photons with $\boldsymbol{E}$ perpendicular to the x axis:

$$\Phi_{\perp}(\alpha, \varphi, \Theta) = \sigma_0 I_{\perp}(\cos\alpha \sin\varphi \sin\Theta + \sin\alpha \cos\Theta)^2 . \tag{B2}$$

Assuming a uniform distribution of chromophores over φ, the average rates of photon absorption for a fixed Θ are obtained by integration of Eqs. (B1) and (B2):

$$\langle\Phi_{\parallel}(\alpha, \varphi, \Theta)\rangle_{\varphi} = (1/2)\sigma_0 I_{\parallel} \sin^2\Theta \tag{B3}$$

$$\langle\Phi(\alpha, \varphi, \Theta)\rangle_{\varphi} = \sigma_0 I_{\perp}(\tfrac{1}{2}\cos^2\alpha \sin^2\Theta + \sin^2\alpha \cos^2\Theta) . \tag{B4}$$

Further averaging over α, assuming a uniform distribution of channels over the axon membrane, yields:

$$q_{\parallel} = (1/2)\sigma_0 I_{\parallel} \sin^2\Theta \tag{B5}$$

$$q_{\perp} = (1/2)\sigma_0 I_{\perp}[\cos^2\Theta + (1/2)\sin^2\Theta] . \tag{B6}$$

Acknowledgments. We thank W. Stuehmer for having kindly provided the programs for stimulation and data acquisition. The technical collaboration of Mr. G. Boido has been of great help during the experiments. We thank W. Stuehmer and G. Ehrenstein for reading the manuscript.

References

Armstrong CM, Bezanilla F (1977) Inactivation of the sodium channel II. Gating current experiments. J Gen Physiol 70:567–590

Beechem JM, Brand L (1985) Time resolved fluorescence of proteins. Annu Rev Biochem 54:43–71

Benz R, Conti F (1981) Structure of the squid axon membrane as derived from charge pulse relaxation studies in the presence of absorbed lipophilic ions. J Membr Biol 59:91–104

Booth J, Muralt A von, Stampfli R (1950) The photochemical action of ultra-violet light on isolated single nerve fibres. Helv Physiol Pharmacol Acta 8:110–127

Busath D, Waldbillig RC (1983) Photolysis of gramicidin A channels in lipid bilayers. Biochim Biophys Acta 736:28–38

Chandler WK, Meves H (1965) Voltage clamp experiments on internally perfused giant axons. J Physiol (London) 180: 799–820

Conti F (1975) Fluorescent probes in nerve membrane. Annu Rev Biophys Bioeng 4:287–210

Conti F, Fioravanti R, Segal JR, Stuehmer W (1982) Pressure dependence of the sodium currents of squid giant axons. J Membr Biol 69:23–34

Creed D (1984) The photophysics and photochemistry of the near-UV absorbing amino-acids. I-Tryptophan and its simple derivatives. II-Tyrosine and its simple derivatives. III-Cystine and its simple derivatives. Photochem Photobiol 39:537–583

Fox JM (1974a) Selective blocking of the nodal sodium channels by ultraviolet radiation. I. Phenomenology of the radiation effect. Pflügers Arch 351:287–301

Fox JM (1974b) Selective blocking of the nodal sodium channels by ultraviolet radiation. II. The interaction of Ca^{++}, H^{+} and membrane potential. Pflügers Arch 351:302–314

Fox JM (1976) Investigation of the relation between structure and function in myelinated nerve fibers with the aid of ultraviolet radiation. Biophys Struct Mech 2:95–97

Fox JM, Stampfli R (1971) Modification of ionic membrane currents of Ranvier nodes by UV radiation under voltage clamp conditions. Experientia 27:1289–1290

Fox JM, Neumcke B, Nonner W, Stampfli R (1976) Blocking of gating currents by ultraviolet radiation in the membrane of myelinated nerve. Pflügers Arch 364:143–145

Greenblatt RE, Blatt Y, Montal M (1985) The structure of the voltage-sensitive sodium channel: Inferences derived from computer-aided analysis of the *Electrophorus electricus* channel primary structure. FEBS Lett 193:125–134

Guy HR, Seetharamulu P (1986) Molecular model of the action potential sodium channel. Proc Natl Acad Sci USA 83: 508–512

Haydon DA, Requena J, Urban BW (1980) Some effects of aliphatic hydrocarbons on electrical capacity and ionic currents of the squid giant axon membrane. J Physiol (London) 309:229–245

Hodgkin AL, Huxley AF, Katz B (1952) Measurement of current-voltage relations in the giant axon of *Loligo*. J Physiol (Lond) 116:424–448

Hof D, Fox JM (1983) Changes of ultraviolet sensitivity of voltage clamped sodium channels during their potential-induced conductance cycle. J Membr Biol 71:31–37

Hof D, Fox JM (1984) Modification of ultraviolet radiation effects on the membrane of myelinated nerve fibers by sulfhydryl compounds. J Membr Biol 79:1–6

Jones D, Hayon E, Busath D (1986) Tryptophan photolysis is responsible for gramicidin-channel inactivation by ultraviolet light. Biochim Biophys Acta 861:62–66

Kimura JE, Meves H (1979) The effect of temperature on the asymmetrical charge movement in squid giant axon. J Physiol (Lond) 289:479–500

Kosower EM (1985) A structural and dynamic molecular model for the sodium channel of *Electrophorus electricus*. FEBS 182:234–242

Lieberman EM (1967) Structural and functional sites of action of ultraviolet radiations in crab nerve fibers. Exp Cell Res 7:489–518

Moore JW, Cole KS (1963) Voltage clamp techniques. Phys Tech Biol Res 6B:263–321

Noda M, Shimizu S, Tanabe T, Takai T, Kayano T, Ikeda T, Takahashi H, Nakayama H, Kanaoka Y, Minamino N, Kangawa K, Matsuo H, Raftery MA, Hiroe T, Inayama S, Hayashida H, Miyata T, Numa S (1984) Primary structure of *Electrophorus electricus* sodium channel deduced from cDNA sequence. Nature 312:121–127

Noda M, Ikeda T, Kayano T, Suzuki H, Takeshima H, Kurasaki M, Takahashi N, Numa S (1986) Existence of distinct sodium channel messenger RNAs in rat brain. Nature 320:188–192

Oxford GS, Pooler JP (1975) Ultraviolet photoalteration of ion channels in voltage-clamped lobster giant axon. J Membr Biol 20:13–30

Salzberg BM, Bezanilla F (1983) An optical determination of the series resistance in *Loligo*. J Gen Physiol 82:807–817

Schwarz W, Fox JM (1977) Ultraviolet-induced alterations of the sodium inactivation in myelinated nerve fibers. J Membr Biol 36:297–310

Stuehmer W, Almers W (1983) Photobleaching through glass micropipettes: sodium channels without lateral mobility in the sarcolemma of frog skeletal muscle. Proc Natl Acad Sci USA 79:946–950

Villegas GM, Villegas R (1984) Squid axon ultrastructure. Curr Top Membr Transp 22:3–37

Weigele JB, Barchi RL (1980) Ultraviolet irradiation produces loss of saxitoxin binding to sodium channels in rat synaptosomes. J Neurochem 35:430–435

Weiss RE, Roberts WM, Stuehmer W, Almers W (1986) Mobility of voltage-dependent ion channels and lectin receptors in the sarcolemma of frog skeletal muscle. J Gen Physiol 87: 955–983

Wetlaufer DB (1962) Ultraviolet absorption spectra of proteins and amino acids. Adv Protein Chem 17:303–390